Akt activation increases cellular cholesterol by promoting the proteasomal degradation of Niemann–Pick C1

Ximing Du*[1, 2], Yuxi Zhang*[1], Sae Rom Jo*, Xiaoyun Liu*, Yanfei Qi*, Brenna Osborne†‡, Frances L. Byrne*, Greg C. Smith†, Nigel Turner†, Kyle L. Hoehn*, Andrew J. Brown* and Hongyuan Yang*[2]

*School of Biotechnology and Biomolecular Sciences, the University of New South Wales, Sydney, NSW 2052, Australia
†School of Medical Sciences, the University of New South Wales, Sydney, NSW 2052, Australia
‡Diabetes & Obesity Research Program, Garvan Institute of Medical Research, Darlinghurst, NSW 2010, Australia

Null mutations of the Niemann–Pick type C1 (*NPC1*) gene cause NPC disease, a lysosomal storage disorder characterized by cholesterol accumulation in late endosomes (LE) and lysosomes (Ly). Nascent or mutated NPC1 is degraded through the ubiquitin–proteasome pathway, but how NPC1 degradation is regulated remains currently unknown. In the present study, we demonstrated a link between NPC1 degradation and the Akt (protein kinase B)/mTOR [mammalian (or mechanistic) target of rapamycin] signalling pathway in cervical cancer cell lines. We provided evidence that activated Akt/mTOR pathway increased NPC1 degradation by ∼50 % in C33A cells when compared with SiHa or HeLa cells. NPC1 degradation in C33A cells was reversed when Akt/mTOR activation was blocked by specific inhibitors or when mTORC1 (mTOR complex 1) was disrupted by regulatory associated protein of mTOR (Raptor) knockdown. Importantly, inhibition of the Akt/mTOR pathway led to decreased NPC1 ubiquitination in C33A cells, pointing to a role of Akt/mTOR in the proteasomal degradation of NPC1. Moreover, we found that NPC1 depletion in several cancer cell lines inhibited cell proliferation and migration. Our results uncover Akt as a key regulator of NPC1 degradation and link NPC1 to cancer cell proliferation and migration.

Key words: cancer, cholesterol, C-terminus of Hsc70-interacting protein (CHIP), mechanistic target of rapamycin (mTOR), Niemann–Pick type C1 (NPC1), ubiquitination.

INTRODUCTION

Niemann–Pick type C (NPC) disease is a progressive neurodegenerative disorder with no effective treatments and no cure [1,2]. NPC is characterized by cholesterol accumulation in late endosomes (LE) and lysosomes (Ly) and approximately 95 % of NPC cases are caused by null mutations of the *NPC1* gene, which encodes a 1278-amino-acid polytopic membrane protein [3,4]. NPC1 localizes to the LE/Ly membrane, where it serves as a key regulator of intracellular cholesterol trafficking [5]. NPC1 mutations lead to the sequestration of low-density-lipoprotein-derived free cholesterol in LE/Ly and subsequent impaired control of cellular cholesterol homoeostasis [6].

To date, hundreds of disease-causing mutations have been identified in the *NPC1* gene, with the most prevalent being that encoding NPC1^{I1061T} [7]. The NPC1^{I1061T} mutant is recognized as a misfolded protein by the endoplasmic reticulum (ER) quality control machinery and consequently targeted for proteasomal degradation [8]. A recent study indicated that the ER-associated degradation of NPC1 requires the E3 ligase CHIP (C-terminus of Hsc [heat shock cognate protein] 70-interacting protein) and involves the ER chaperone heat-shock proteins [9]. Besides mutated NPC1 such as the NPC1^{I1061T}, at least half of wild-type (WT) NPC1 is believed to be retained in the ER and undergoes ER-associated degradation [8]. However, it remains unclear how the degradation of NPC1 is regulated and whether any other factors are involved.

The serine/threonine kinase Akt (protein kinase B) is frequently activated in various human cancers, contributing to cancer cell survival and proliferation [10]. The activation of Akt is growth-factor-responsive and phosphoinositide-3-kinase (PI3K) -dependent [10]. An activated form of Akt bears the two active residues being sequentially phosphorylated: Thr^{308} by phosphoinositide-dependent protein kinase-1 [11] and Ser^{473} by mammalian (or mechanistic) target of rapamycin (mTOR) complex 2 (mTORC2) [12,13]. Activated Akt then phosphorylates various substrates involved in cell metabolism, survival and cell cycle [14]. Significantly, Akt signalling increases the amount of cellular free cholesterol, which is needed for growing and dividing cells, by activating sterol-regulatory-element-binding proteins (SREBPs), the master transcriptional regulators of cholesterol metabolism [15].

In the present study, we uncovered a novel link between Akt signalling and NPC1 degradation: the level of NPC1 was specifically reduced in cancer cell lines with highly active Akt. We demonstrated that Akt activation is both necessary and sufficient for NPC1 degradation in cancer cell lines. Our results reveal a novel mechanism by which certain cancer cells accumulate cholesterol and link NPC1 to optimal cancer proliferation and migration.

EXPERIMENTAL

Materials

Dulbecco's modified Eagle's medium (DMEM), penicillin/streptomycin and Dulbecco's PBS were obtained from Life

Abbreviations: CA-Akt, constitutively active Akt; CHIP, C-terminus of Hsc70-interacting protein; DMEM, Dulbecco's modified Eagle's medium; ER, endoplasmic reticulum; EV, empty vector; GPAT, glycerol-3-phosphate acyltransferase; LAMP1, lysosome-associated membrane protein 1; LE, late endosome(s); Ly, lysosome(s); mTOR, mammalian (or mechanistic) target of rapamycin; mTORC, mTOR complex; NPC, Niemann–Pick type C; ORP5, oxysterol-binding protein-related protein 5; PI3K, phosphoinositide 3-kinase; Raptor, regulatory associated protein of mTOR; Rictor, rapamyc-ininsensitive companion of mTOR; S6K, S6 kinase; SLP1, stomatin-like protein-1; WT, wild-type.

[1] These authors contributed equally to this work.

[2] Correspondence may be addressed to either of these authors (email x.r.du@unsw.edu.au or h.rob.yang@unsw.edu.au).

Technologies Australia. FBS was obtained from Bovogen Biologicals. Filipin, MG132 (MG stands for MyoGenetics), LY294002, chloroquine, rapamycin, glycerol and protease inhibitor cocktail were obtained from Sigma–Aldrich. All oligonucleotides were obtained from IDT (Integrated DNA Technologies) with standard desalting.

Cell culture and transfection

HeLa, SiHa, C33A, Huh7, HEC-1-A (HEC), RL95-2 (RL) cells were obtained originally from A.T.C.C. (SiHa and C33A cells were kindly provided by Dr Noel Whitaker, the University of New South Wales, Sydney, Australia); Ishikawa cells (ISH) were obtained from Sigma–Aldrich; MFE-296 (296) cells were obtained from Deutsche Sammlung von Mikroorganismen und Zellkulturen (DSMZ). Monolayers of cells were maintained in DMEM supplemented with 10 % FBS, 100 units/ml penicillin and 100 μg/ml streptomycin sulfate in 5 % CO_2 at 37 °C. DNA transfection was performed using Lipofectamine™ LTX and Plus Reagent (Life Technologies) according to the manufacturer's instruction. siRNA transfection was carried out in cells grown in full serum medium according to standard methods using Lipofectamine™ RNAiMAX transfection reagent (Life Technologies).

Antibodies

We obtained all antibodies from Cell Signaling Technology, except rabbit polyclonal antibody against the C-terminal region of human NPC1 (Abcam), mouse monoclonal antibodies against LAMP1 (lysosome-associated membrane protein 1; Santa Cruz Biotechnology), NPC2 (Santa Cruz Biotechnology), actin (Abcam), Flag (Sigma–Aldrich) and GFP (Santa Cruz Biotechnology). For immunoblotting, we obtained horseradish peroxidase-conjugated secondary antibodies from Jackson ImmunoResearch. For immunofluorescence, we obtained Alexa Fluor-conjugated secondary antibodies from Molecular Probes/Life Technologies.

Constructs

Myc–Akt DE (S477D, T479E) and Myc–Akt DDE (S473D, S477D, T479E) were generated from Myc–WT-Akt and Myc–CA (constitutively active)-Akt (S473D) [16] respectively, by site-directed mutagenesis. pCMV (cytomegalovirus)-NPC1-mCherry was generated by subcloning of mouse NPC1 from pCMV-NPC1-YFP [17] into pCMV-mCherry-N1 vector. pCMV-NPC1-HA (hemagglutinin) and pCMV-NPC1-Flag were generated from pCMV-NPC1-mCherry by swapping the mCherry tag with HA and Flag tags respectively. pCMV-GFP-SLP1 (stomatin-like protein-1) was kindly provided by Dr Bao-Liang Song (College of Life Sciences, Wuhan University, Wuhan, China). pCMV-GFP-ORP5 (oxysterol-binding protein-related protein 5) and pCMV-YFP-LAMP1 were previously described [18]. Mouse version of pCMV6-GPAT3 (glycerol-3-phosphate acyltransferase 3)-Flag and pCMV6-GPAT4-Flag were obtained from OriGene.

siRNAs

We obtained siRNAs from GenePharma or Sigma–Aldrich. Targeting sequences of siRNAs against NPC1were siNPC1.1, 5′-CUCCCAUCGAUAGCAAUA-3′, siNPC1.2, 5′-GAGGUACAAUUGCGAAUA-3′ and siNPC1.3, 5′-GCUGUCGAGUGGACAAUA; against CHIP was siCHIP, 5′-GGAGCAGGGCAAUCGUCU-3′ [9], against regulatory associated protein of mTOR (Raptor) was siRaptor, 5′-GCGUCACACUGGAUUUGA-3′; against rapamycin-insensitive companion of mTOR (Rictor) was siRictor, 5′-GCCAAAGUUUCAAUACAG-3′.

Quantitative real-time reverse transcription-PCR

Total RNA was extracted using TRIzol (Life Technologies). cDNA was generated from total RNA using a SuperScript VILO cDNA Synthesis Kit (Life Technologies). PCR was performed using Rotor-Gene RG-3000A (Qiagen). Threshold cycle value for each gene was acquired at the exponential phase and transcript expression levels were normalized to β-actin using Δ_{CT} values. We used the following primers purchased from GeneWorks or Sigma–Genosys (listed 5′ to 3′ in the order of forward primer, reverse primer): β-actin, 5′-AGCGAGCATCCCCCAAAGTT-3′ (forward) and 5′-GGGCACGAAGGCTCATCATT-3′ (reverse); NPC1, 5′-CAGTCTCTGTTGTGATGTTCGG-3′ (forward) and 5′-CTGACTCTGTCGAGGGCTACA-3′ (reverse).

Immunoblot analysis

Immunoblot analysis was performed as previously described [18]. Briefly, samples were mixed with 2× Laemmli buffer, boiled for 5 min at 95 °C or incubated for 10 min at 70 °C and then subjected to SDS/PAGE (7.5 % or 10 % gel). After electrophoresis, the proteins were transferred to Hybond-C nitrocellulose filters (GE Healthcare). Incubations with primary antibodies were performed at 4 °C overnight. Secondary antibodies were horseradish peroxidase-conjugated AffiniPure donkey anti-rabbit or donkey anti-mouse IgG (H + L; Jackson ImmunoResearch Laboratories) used at a 1:5000 dilution. The bound antibodies were detected by ECL Western blotting detection reagent (GE Healthcare or Merck Millipore) and visualized with Molecular Imager® ChemiDocTM XRS + (Bio-Rad Laboratories).

Filipin staining, immunofluorescence and confocal microscopy

Cells grown on coverslips were fixed with 4 % paraformaldehyde for 30 min at room temperature. Cells were stained with freshly prepared 50 μg/ml filipin in PBS for 1 h at room temperature. Stained cells were imaged using a Leica CTR5500 microscope equipped with an EL6000 fluorescent lamp and a DFC300 FX digital camera. Quantification of filipin intensities was carried out as previously described [18]. Immunofluorescence was carried out as previously described [19]. Cells were mounted in ProLong® Gold antifade reagent (Life Technology). Confocal images were acquired on an Olympus FV1200 laser-scanning microscope. The manufacturer's software and FIJI software were used for data acquisition and analysis.

Cholesterol measurement

The content of total and free cholesterol in cell lysates was measured using Wako kits according to the manufacturer's instruction.

Immunoprecipitation for ubiquitination assay

After transfection and treatment, cells grown in 100-mm dishes were harvested, washed with cold PBS, resuspended in 1 ml of cell lysis buffer (50 mM Tris/HCl, pH 7.8, 100 mM NaCl and 1 % Triton X-100) containing Protease Inhibitor Cocktail (100×, Sigma) and Phosphatase Inhibitor Cocktail (100×, Cell Signaling Technology). Cell lysates were passed through a

22-gauge needle 20 times, incubated on ice for 30 min and clarified by centrifugation at 18000 *g* for 15 min at 4 °C. Immunoprecipitation of the lysates with a polyclonal antibody against NPC1 was performed using Dynabeads®–Protein G (Life Technologies) according to manufacturer's instructions. The immunoprecipitated pellets were resuspended in 60 μl of 2× Laemmli buffer (Sigma–Aldrich) and then incubated for 10 min at 70 °C. The resultant samples were subjected to SDS/PAGE and immunoblotting.

MTS assay

HeLa cells were seeded in 96-well plates at 2.5×10^3 cells/well and transfected with siRNA (20 nM) for 72 h. Six wells were seeded for each transfection. Cell proliferation was measured with a MTS assay kit (CellTiter 96® AQueous One Solution Cell Proliferation Assay, Promega). For each reading, 20 μl of MTS solution was added, plates were incubated for 1–2 h, and absorbance was read on a Spectra MAX340 Microplate Reader at 490 nm.

Cell migration assay

HeLa cells were seeded in a 24-well plate containing Culture-Insert 24 (Ibidi® cells in focus) and transfected with control siRNA or siNPC1 for 24 h. After Culture-Insert was removed, the image was taken at 0 and 24 h using an Olympus CKX41 microscope fitted with an Infinity 1-2CB camera (Lumenera Corporation) connected to a computer. Percentage cell migration was quantified using NIH ImageJ software. Data from 24 h were normalized to those of 0 h.

FACS

C33A cells transfected with empty vector (EV; pCMV–mCherry or pCMV–NPC1–mCherry) were sorted with a BD Influx Cell Sorter (BD Biosciences) using the cell sorting service of the Flow Cytometry Facility, Biological Resources Imaging Laboratory (Mark Wainwright Analytical Centre, University of New South Wales) to obtain enriched live fluorescent cells. The sorted cells were expanded and used for the MTS assay.

Statistical analyses

Statistical analysis between groups was performed using Prism 6 for Windows version 6.03 (GraphPad Software) with unpaired Student's *t* tests or one-way ANOVA. Data are expressed as means + S.D. unless otherwise stated. Significant differences are indicated in the figures.

RESULTS

Free cholesterol is accumulated in C33A cells with reduced NPC1

We analysed free cholesterol distribution by filipin, a fluorescent dye that specifically binds to cholesterol, in six common cancer cell lines to examine whether there is any aberrant intracellular cholesterol trafficking in these cells. We found that ~60–70 % of C33A cells (a human papillomavirus-negative human cervical carcinoma cell line) grown in full serum culture medium accumulated large amount of free cholesterol (Supplementary Figure S1). In contrast, SiHa and HeLa cells (human papillomavirus-16-positive human cervical cancer cell lines) displayed little intracellular cholesterol accumulation (Supplementary Figure S1; Figure 1A). An enzymatic colorimetric assay further showed that both free and total cholesterol contents in C33A cells were significantly higher than in SiHa cells (Figure 1B). Interestingly, cholesterol was accumulated in LAMP1 (LE/Ly marker)-positive compartments in C33A cells (Figure 1C). This phenotype is reminiscent of NPC disease, which is characterized by free cholesterol accumulation in LE/Ly [2]. More than 95 % of all NPC cases are caused by mutations in the *NPC1* gene [3]. As expected, NPC1 protein, but not mRNA, was dramatically reduced in C33A cells when compared with SiHA cells (Figures 1D–1F) and, more importantly, cholesterol accumulation in C33A cells was reduced by overexpression of NPC1 tagged with mCherry (Figure 1G). Because *NPC1* mRNA levels were quantitatively similar between C33A and SiHa cells (Figure 1F), we next mainly focused on the regulation of NPC1 degradation in C33A cells.

NPC1 degradation in C33A cells is associated with Akt activation

At steady state and consistent with a previous report [20], C33A cells, but not SiHa or HeLa cells, had highly activated Akt as indicated by the detection of Akt phosphorylation on Ser^{473} (Figures 2A and 2B). This was accompanied by a nearly 50 % reduction in NPC1 in C33A cells (Figures 2A and 2B). The association between NPC1 and phosphorylated Akt was also seen in endometrial cancer cell lines [21]: NPC1 levels were reduced in cells with activated Akt (ISH, 296, RL) when compared with HEC cells with a much lower level of Akt activation (Figure 2C). These data strongly suggested that there is a specific link between NPC1 degradation and Akt activation. Indeed, when C33A cells were treated with a PI3K inhibitor, LY294002, Akt activation was inhibited and NPC1 levels were increased by 50 % (Figure 2D, left). In contrast, LY294002 had no effect on NPC1 in cells without activated Akt (SiHa cells) (Figure 2D, right). Similar results were observed when cells were treated MK-2206, an allosteric inhibitor of Akt, which potently blocked Akt Ser^{473} phosphorylation and increased NPC1 2-fold in C33A cells (Figure 2E).

To test whether Akt activation is sufficient to reduce NPC1, we co-transfected HeLa cells with cDNAs encoding NPC1 tagged with mCherry at the C-terminus and c-Myc-tagged CA-Akt (S473D) [16] (Figure 3A). NPC1–mCherry was decreased in a manner dependent on the expression of Myc–CA-Akt, with the highest level of CA-Akt expression inducing the strongest reduction in NPC1–mCherry (Figure 3A, lane 5). A recent study revealed that Akt activation was regulated by cell cycle and phosphorylation of the two amino acids at the Akt extreme C-terminus (Ser^{477} and Thr^{479}) promoted Akt Ser^{473} phosphorylation [22]. Therefore, we constructed another two forms of CA-Akt: Myc–Akt DE and Myc–Akt DDE, by mutating S477D and T479E from WT-Akt and Myc—CA-Akt (S473D) respectively. Overexpression of both Akt DE and Akt DDE mutants promoted robust Akt Ser^{473} phosphorylation and reduced the expression of both NPC1–HA and NPC1–Flag (Figure 3B, lanes 2, 3, 5 and 6). This effect appeared to be specific to NPC1 as the expression of the other four membrane proteins, GFP-tagged SLP1 [23] and ORP5 [18], as well as Flag-tagged GPAT3 and GPAT4, two ER membrane-associated enzymes [24], were unchanged or even increased when co-expressed with Akt DE or Akt DDE mutants [Figure 3C (lanes 4–9) and 3D (lanes 4–9)]. We also compared the turnover of LAMP1 with that of NPC1. LAMP1 and NPC1 co-localize at LE/Ly [19]. When co-expressed with Akt DE, the level of YFP-tagged NPC1 was strongly reduced, whereas YFP-tagged LAMP1 was generally stable (Supplementary Figure S2), further suggesting that this phenomenon is protein-specific rather than organelle-specific.

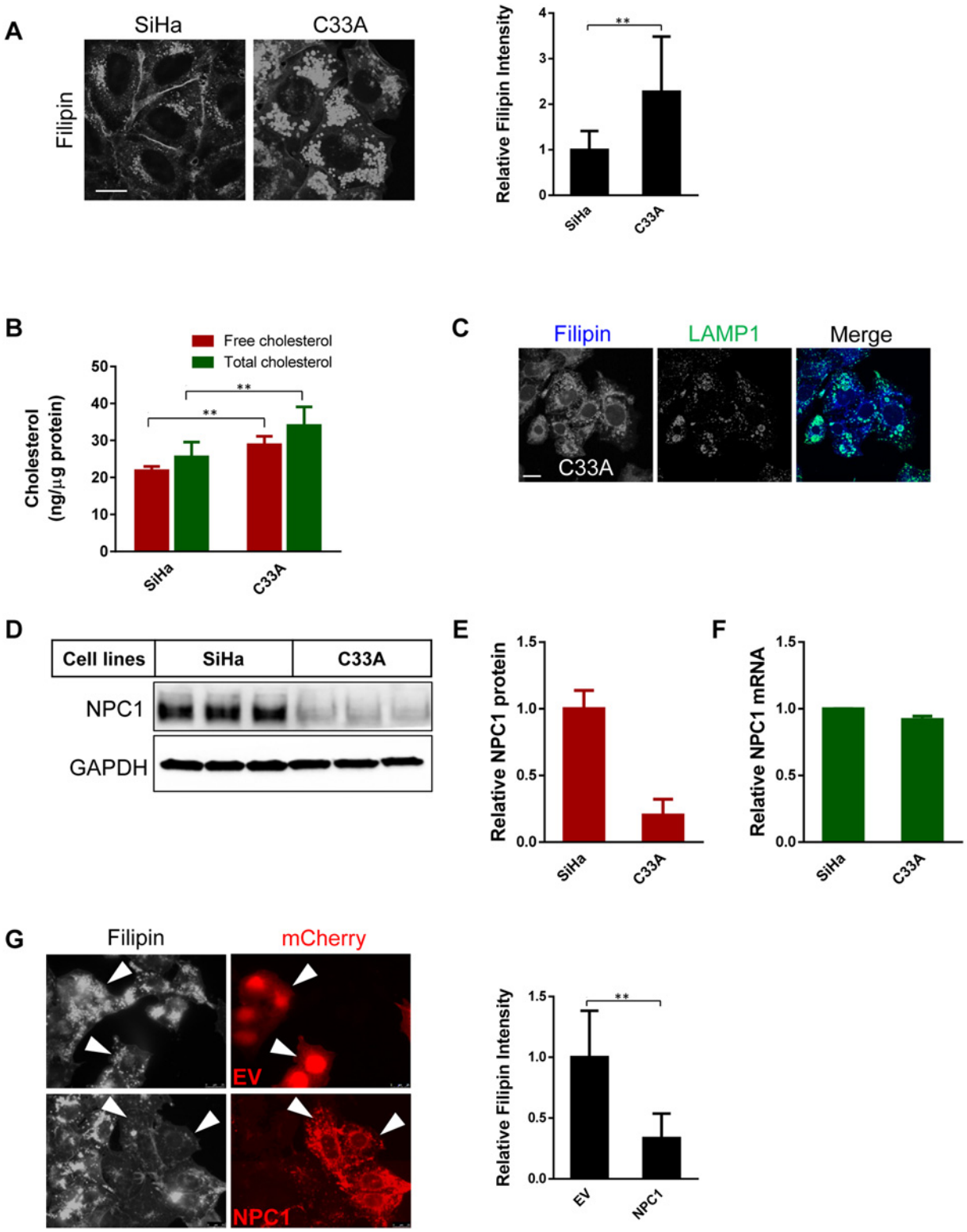

Figure 1 Free cholesterol is accumulated in C33A cells with down-regulated NPC1

(**A**) Filipin staining of free cholesterol indicates cholesterol accumulation in C33A but not in SiHa cells. Quantification of filipin intensity is shown in the right panel. (**B**) Biochemical measurement of free cholesterol content in C33A and SiHa cells, $^{**}P < 0.01$. (**C**) Co-localization of accumulated cholesterol in C33A cells with the late endosomal/lysosomal marker, LAMP-1. (**D**) Immunoblotting of NPC1 in C33A and SiHa cells. (**E**) Densitometry of NPC1 levels normalized to those of GAPDH presented in (**D**). (**F**) Quantitative PCR shows no difference of *NPC1* mRNA levels between C33A and SiHa cells. (**G**) Filipin staining of C33A cells transfected with either mCherry EV or mCherry-tagged NPC1 for 24 h. Quantification of filipin intensity in EV- or NPC1–mCherry-expressing cells is shown in the right panel.

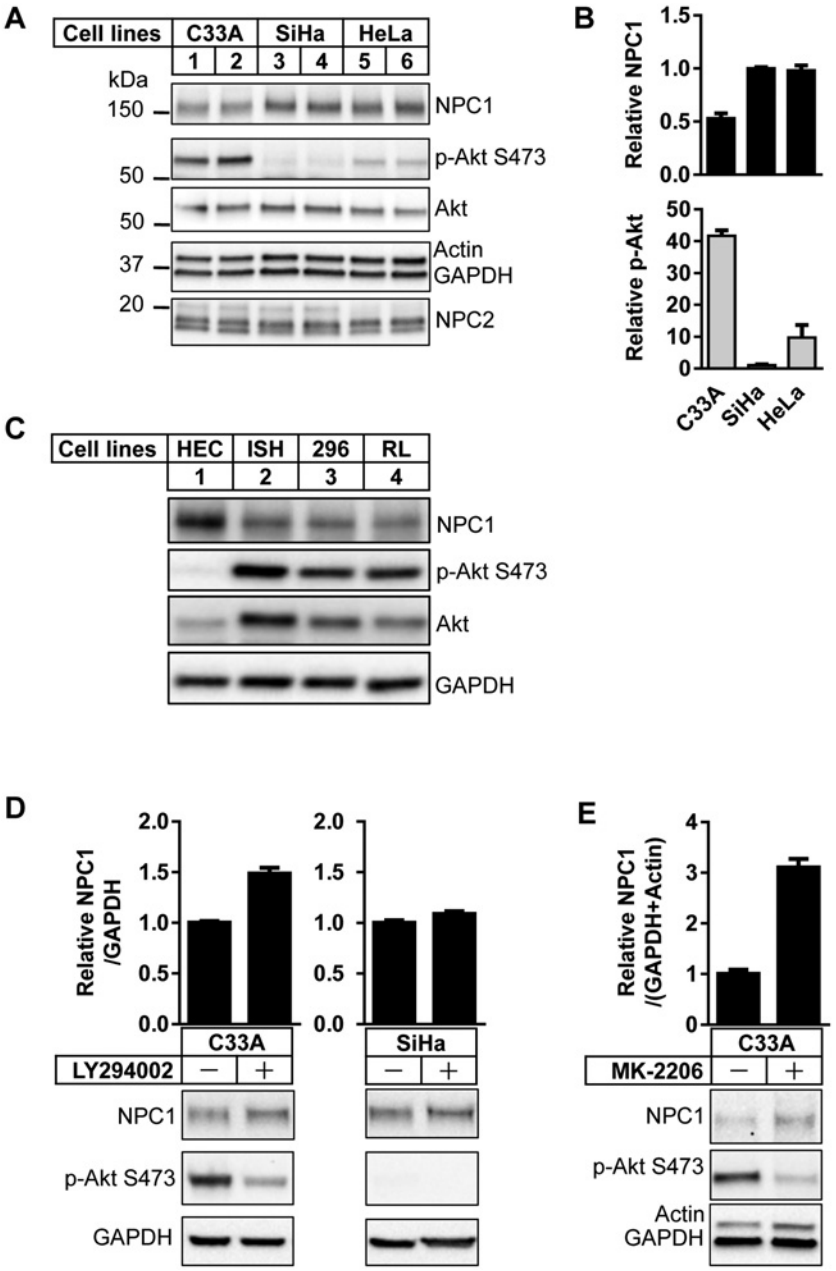

Figure 2 NPC1 degradation in C33A cells is associated with Akt activation

(**A**) Immunoblotting analysis of NPC1, p-Akt Ser^{473}, total Akt and NPC2 in C33A, SiHa and HeLa cells. (**B**) Relative amounts of NPC1 or p-Akt/Akt were quantified based on results in (**A**). The values normalized to actin and GAPDH for SiHa cells were set as 1. (**C**) Immunoblotting analysis of NPC1, p-Akt Ser^{473} and total Akt in in endometrial cancer cells. (**D** and **E**) Immunoblotting analysis of NPC1 and p-Akt Ser^{473} in C33A or SiHa cells were treated with 20 μM LY294002 (**D**) or 1 μM MK-2206 (**E**) for 16 h. Relative NPC1 normalized to GAPDH/actin were quantified from at least two separate experiments.

Next, we tested whether mTOR, a major down stream target of the PI3K/Akt pathway [25], plays any role in Akt-mediated NPC1 degradation. When C33A cells were treated with rapamycin, a specific inhibitor of mTOR, the level of NPC1 was similarly increased when compared with those cells treated with the Akt inhibitor MK-2206 (Figures 4A and 4B). mTOR is a conserved component forming two functionally distinct complexes, mTORC1 and mTORC2 [25]. In the short-term, rapamycin specifically inhibits mTORC1 by targeting another component of mTORC1, Raptor [26]. To test whether knocking down Raptor to inhibit mTORC1 function has similar effects to that of rapamycin, we treated C33A cells with siRNAs against Raptor, as well as NPC1, which was included as a positive control and Rictor, a major component of mTORC2 [27]. Although NPC1 siRNA almost completely depleted NPC1 and Rictor siRNA had little effect, Raptor knockdown increased NPC1 levels by more than 75 % compared with control cells [Figures 4C (lane 4) and 4D]. These data strongly suggest that mTORC1 and not mTORC2 is involved in PI3K/Akt pathway-mediated NPC1 degradation.

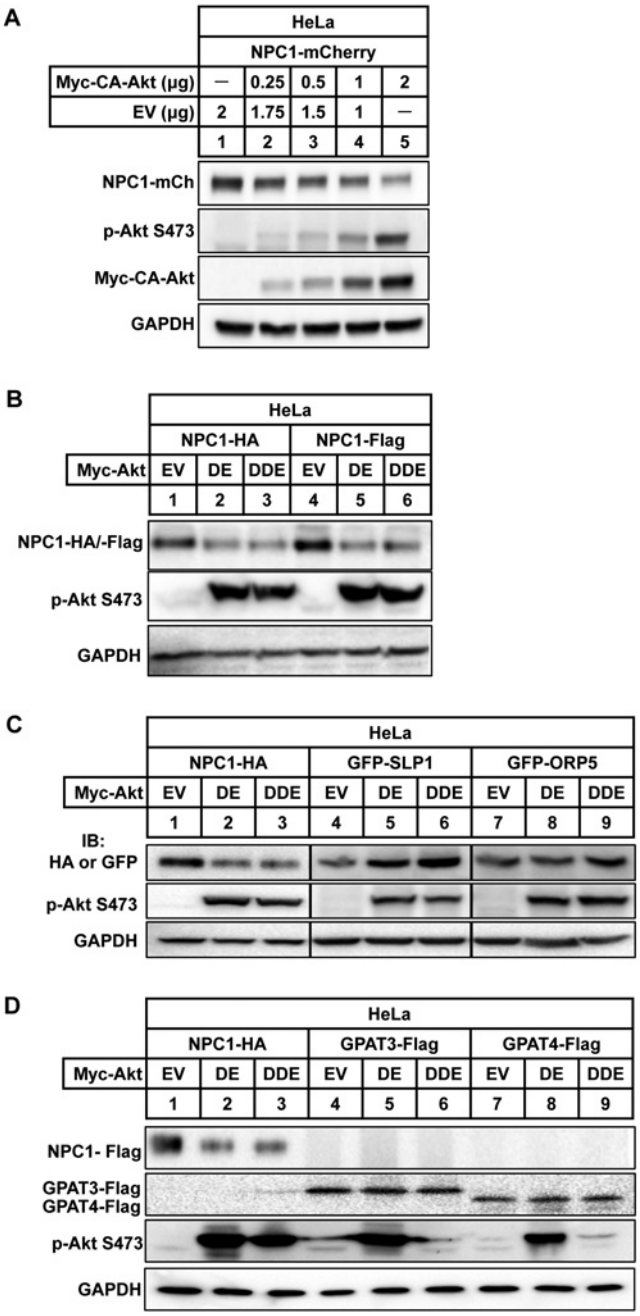

Figure 3 CA-Akt promotes NPC1 degradation

(**A**) HeLa cells were transfected with cDNAs encoding NPC1–mCherry and different amounts of Myc–CA-Akt or EV for ∼24–48 h. Total cell lysates were analysed by immunoblotting to detect NPC1, p-Akt Ser^{473} or Myc–CA-Akt. (**B**) HeLa cells were co-transfected with indicated cDNAs encoding HA- or Flag-tagged NPC1, Myc–Akt DE, Myc–Akt DDE or EV for 24–48 h. Total cell lysates were analysed by immunoblotting to detect NPC1, p-Akt Ser^{473}. (**C**) HeLa cells were co-transfected with indicated cDNAs encoding Myc–Akt DE, Myc–Akt DDE or EV together with HA-tagged NPC1 or GFP-tagged SLP1 or GFP-tagged ORP5 for 24–48 h. Total cell lysates were analysed by immunoblotting to detect NPC1 or p-Akt Ser^{473}. All results are representative of at least two independent experiments with similar results. (**D**) HeLa cells were co-transfected with the indicated cDNAs encoding Myc–Akt DE, Myc–Akt DDE or EV together with HA-tagged NPC1 or Flag-tagged GPAT3 or GPAT4 for 24–48 h. Total cell lysates were analysed by immunoblotting to detect NPC1, GPAT3/4–Flag or p-Akt Ser^{473}. All results are representative of at least two independent experiments with similar results.

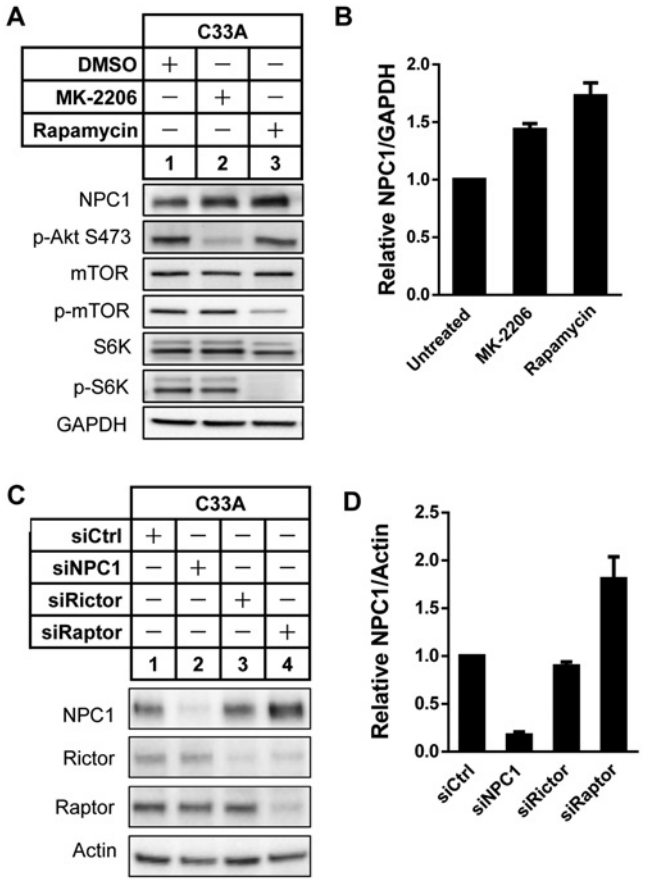

Figure 4 Inhibition of the Akt/mTOR pathway blocks NPC1 degradation

(**A**) C33A cells were treated with MK-2206 (1 μM), rapamycin (1 μM) or DMSO alone for 16 h. Total cell lysates were analysed by immunoblotting to detect NPC1 and other proteins as indicated. (**B**) Relative NPC1 in (**A**) normalized to GAPDH (glyceraldehyde-3-phosphate dehydrogenase). (**C**) C33A cells were treated with indicated siRNAs for 72 h and total cell lysates were analysed by immunoblotting. (**D**) Relative NPC1 in (**C**) normalized to actin. Results are representative of at least two independent experiments with similar results.

Akt/mTORC1 mediates NPC1 degradation through the ubiquitin–proteasome pathway

It has been shown that NPC1 can be ubiquitinated and subsequently degraded by the proteasomal pathway [8,9]. Consistent with the previous study [8], we found that treatment with glycerol, a chemical chaperone that stabilizes misfolded proteins [28], and the proteasome inhibitor MG132 strongly increased the level of NPC1 in C33A cells (Figures 5A–5C). As a result, MG132 treatment reduced cholesterol accumulation in C33A cells as indicated by filipin staining (Figure 5D). Also consistent with the previous study [8], treatment with chloroquine, a lysosomal inhibitor that prevents the degradation of the autophagic protein [29], decreased the level of NPC1 (Figure 5C, lane 3), further demonstrating that NPC1 is proteasomally degraded in C33A cells. Disruption of the PI3K/Akt/mTORC1 pathway may interfere with NPC1 degradation by the ubiquitin–proteasome pathway, thereby increasing the level of NPC1. To test this hypothesis, we treated C33A cells with control siRNA or Raptor siRNA, followed by the transfection of the cDNA for HA-tagged ubiquitin. Before harvest, cells received MG132 treatment for 6 h and cell lysates were subjected to immunoblotting analysis or immunoprecipitation with anti-NPC1 antibody (Figure 6A). MG132 treatment caused

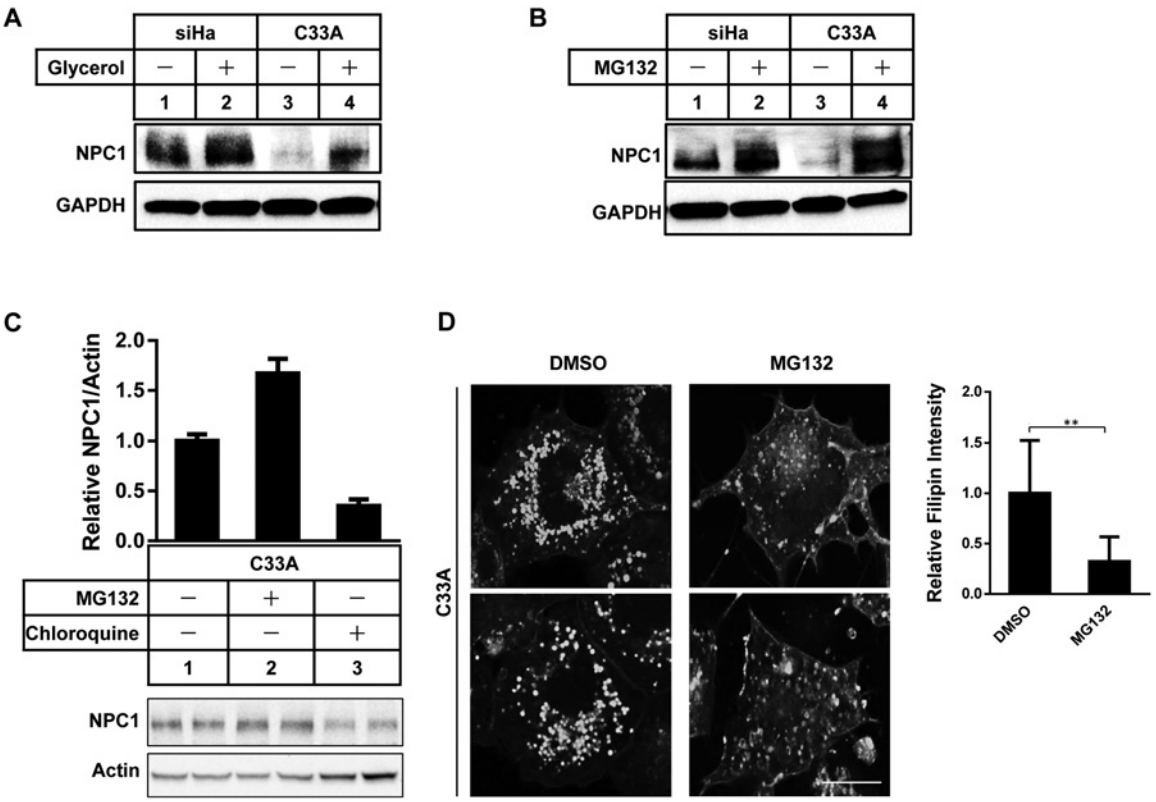

Figure 5 NPC1 is degraded by the proteasomal pathway in C33A cells

(**A**) SiHa and C33A cells were treated with glycerol (10 %, v/v), for 24 h. Total cell lysates were analysed by immunoblotting to detect NPC1 and GAPDH (glyceraldehyde-3-phosphate dehydrogenase). (**B**) SiHa and C33A cells were treated with MG132 (10 μM) for 16 h. Total cell lysates were analysed by immunoblotting to detect NPC1 and GAPDH. (**C**) C33A cells were treated with MG132 (10 μM) or chloroquine (50 μM) for 16 h. Total cell lysates were analysed by immunoblotting to detect NPC1. Relative NPC1 normalized to actin is shown. (**D**) C33A cells were treated with MG132 (10 μM) for 16 h. Cells were stained with fillipin for free cholesterol. Quantification of filipin intensity is shown in the right panel. Note that MG132-treated cells had a reduced level of accumulated cholesterol.

a robust accumulation of NPC1 in both control and Raptor siRNA-treated cells (Figure 6A, lanes 3 and 4). Analysis of NPC1 immunoprecipitates in the presence of MG132 clearly showed that the ubiquitination of NPC1 was decreased when Raptor was down-regulated by siRNA (Figure 6A, lane 6). Similarly, MG132 also caused the accumulation of NPC1 when cells were treated with or without the dual PI3K/mTOR inhibitor PI-103 (PI3K inhibitor-103) (Figure 6B, lanes 3 and 4). When the PI3K/Akt/mTOR pathway was shut down by PI-103, the level of NPC1 was increased (Figure 6B, lane 2) and NPC1 ubiquitination was also decreased in the presence of MG132 (Figure 6B, lane 10). Importantly, it appeared that in C33A cells depleting CHIP, an E3 ligase for NPC1 [9], increased NPC1 level in the absence of MG132 (Figure 6C, lane 2) and reduced NPC1 ubiquitination in the presence of MG132 (Figure 6C, lane 8). Taken together, these data support the notion that the PI3K/Akt/mTORC1 pathway promotes NPC1 turnover through the ubiquitin–proteasome system.

Depletion of NPC1 impairs cancer cell proliferation and migration

Cell growth and proliferation is mainly regulated by the PI3K/Akt/mTOR pathway, which is often dysregulated in cancer due to many factors, such as mutation, deletion and post-translational modifications [30]. It is possible that the down-regulation of NPC1 by the PI3K/Akt/mTORC1 pathway may be linked to cell growth and proliferation. To test this possibility, we assayed cell proliferation using a colorimetric assay of MTS, one of the tetrazolium compounds that changes colour due to the intracellular reductive products in proportion to the number of cells. First, we compared C33A and SiHa cells and found that C33A cells, which had markedly low levels of NPC1 (Figures 1D and 2A), showed significantly reduced cellular proliferation as indicated by the MTS colorimetric assay (Figure 7A). Importantly, the MTS assay showed that overexpression of NPC1 in C33A cells enhanced cell proliferation (Supplementary Figure S3). Next, we transiently depleted NPC1 by three different siRNAs and carried out the MTS assay in HeLa cells. All three NPC1 siRNAs efficiently knocked down NPC1 (Figure 7B), which was verified by resultant free cholesterol accumulation in these cells as revealed by filipin staining (Figure 7C). The MTS assay indicated a significant decrease (~40 %) in cell proliferation in HeLa cells with NPC1 silenced (Figure 7D). Moreover, the cell migration assay showed that NPC1 depletion suppressed HeLa cell migration by ~50 % (Figures 7E and 7F). Similar results were seen in SiHa cells as well as in Huh7 cells, a human hepatoma cell line (Supplementary Figure S4). Likewise, NPC1 knockdown significantly inhibited both Huh7 and SiHa cell proliferation (Supplementary Figures S4B and S4F) and Huh7 cell migration (Supplementary Figures S4C and S4D). These data indicate that NPC1 is required for optimal cell growth and migration in certain cancer cells.

DISCUSSION

In the present study, we demonstrated that an active PI3K/Akt/mTOR pathway promotes NPC1 degradation, which

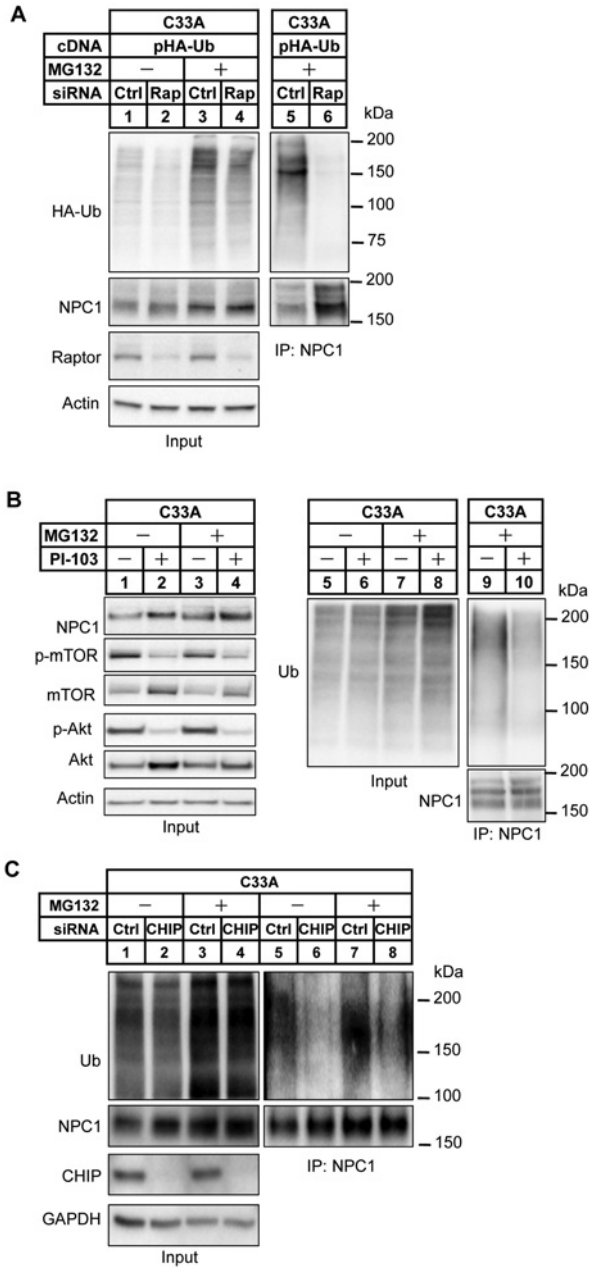

Figure 6 The Akt/mTOR pathway regulates NPC1 degradation via the ubiquitin–proteasome pathway

(**A**) C33A cells were treated with control siRNA or siRaptor for 24 h, followed by the transfection with cDNA encoding HA-tagged ubiquitin (pHA-UB) for 24 h. Cells were then incubated in the absence or presence of MG132 (10 μM) for 6 h. Total cell lysates (inputs) were analysed by immunoblotting to detect NPC1, Raptor, HA–ubiquitin or actin (lanes 1–4). Cell lysates of same amount of total proteins from MG132-treated cells were immunoprecipitated with anti-NPC1 polyclonal antibody followed by immunoblotting with anti-HA monoclonal and anti-NPC1 antibodies (lanes 5–6). (**B**) C33A cells were either untreated or treated with dual Akt/mTOR inhibitor PI-103 (2 μM) for 16 h, followed by the treatment with or without MG132 (10 μM) for 6 h. Total cell lysates (inputs) were analysed by immunoblotting to detect NPC1, p-mTOR, p-Akt, actin (lanes 1–4) or ubiquitin (lanes 5–8). Cell lysates of same amount of total proteins from MG132-treated cells were immunoprecipitated with anti-NPC1 polyclonal antibody followed by immunoblotting with anti-ubiquitin and anti-NPC1 antibodies (lanes 9 and 10). (**C**) C33A cells were treated with control siRNA or siCHIP for 48 h, followed by treatment with or without MG132 (10 μM) for 6 h. Total cell lysates (inputs) were analysed by immunoblotting to detect ubiquitin, NPC1, CHIP or GAPDH (lanes 1–4). Cell lysates of the same amount of total proteins were immunoprecipitated with anti-NPC1 polyclonal antibody followed by immunoblotting with anti-ubiquitin and anti-NPC1 antibodies (lanes 5–8). All results are representative of three independent experiments with similar results.

accounts for increased cellular free cholesterol in certain cancer cells. The most critical information came from those cancer cells with highly activated Akt (e.g. C33A and endometrial cancer cells). These cells expressed NPC1 at much lower levels than cell lines with minimal Akt activation at steady state (Figures 1 and 2). Importantly, NPC1 reduction in these cells could be reversed when the PI3K/Akt/mTOR pathway was blocked by each of the following inhibitors: LY294001 (PI3K; Figure 2D), MK-2206 (Akt; Figure 2E), rapamycin (mTOR; Figure 4A) or PI-103 (Akt and mTOR; Figure 6B). Secondly, when co-expressed with the CA form of Akt (CA-Akt), the level of mCherry or an epitope (HA or Flag)-tagged NPC1 was significantly reduced (Figure 3). The third piece of evidence was derived from siRNA knockdown experiments where the NPC1 level was significantly increased upon knocking down Raptor (Figure 4C). Together, these results suggest that Akt activation is both necessary and sufficient for NPC1 degradation in cancer cell lines.

Consistent with the previous study [8], we showed that the proteasome inhibitor MG132 increased NPC1 level in C33A cells (Figure 5). In the presence of MG132, Raptor depletion or the dual Akt/mTOR inhibitor PI-103 treatment reduced NPC1 ubiquitination (Figures 6A and 6B), which clearly indicated that NPC1 degradation via the ubiquitin–proteasome pathway is regulated, at least in part, by Akt/mTOR. One possibility is that Akt may target the E3 ubiquitin ligase of NPC1 to regulate its degradation. Dickey et al. [31] reported that Akt and the E3 ligase CHIP physically and functionally interact. This interaction is important for clearance of tau, a microtubule-associated protein and a pathological hallmark of Alzheimer disease. Moreover, a recent study demonstrated that CHIP and NPC1 could be co-precipitated and CHIP ubiquitinated and degraded NPC1 in CV-1 [simians] in origin with SV40 genes (COS) and human embryonic kidney 293 (HEK-293) cells [9]. Therefore, it is possible that a 'superactive' Akt may activate CHIP and promote CHIP–NPC1 interaction, causing NPC1 degradation. Indeed, CHIP depletion appears to reduce NPC1 ubiquitination in C33A cells (Figure 6C). However, the interaction between NPC1 and CHIP could be transient or cell- type-specific, as we could not detect this interaction by co-immunoprecipitation in HeLa or C33A cells. In future studies, it would be important to further examine whether and how CHIP is phosphorylated by Akt and whether the NPC1–CHIP interaction is Akt-dependent in COS or HEK cells.

Another possibility is that Akt may directly phosphorylate NPC1 and promote its degradation. Such a case has been reported for tuberin and forkhead box protein O (FOXO) proteins, which are negative regulators of cell growth and survival, and substrates of Akt [32,33]. Akt activation could phosphorylate these proteins and trigger their ubiquitination and proteasomal degradation [34]. However, there has been no evidence for NPC1 being phosphorylated by Akt. We were also unable to detect any NPC1 phosphorylation using antibodies such as anti-phospho-(serine/threonine) Akt substrate upon activation of Akt (results not shown) [35]. It should be noted that Akt may regulate NPC1 degradation through downstream mTORC1, as rapamycin treatment or Raptor knockdown could reverse NPC1 degradation in C33A cells (Figure 4). We were particularly interested in investigating whether any other factors are involved in this regulation. To this end, we examined p70 S6 kinase (p70 S6K), a downstream effector of the Akt/mTORC1 pathway [25]. However, when the activation of p70 S6K was blocked by specific inhibitors, we did not observe any apparent rescue effect on NPC1 degradation in C33A cells (results not shown).

The findings of the present study raise an intriguing question: why does an activated Akt/mTOR pathway promote NPC1 degradation? Cholesterol is required for the uncontrolled cell

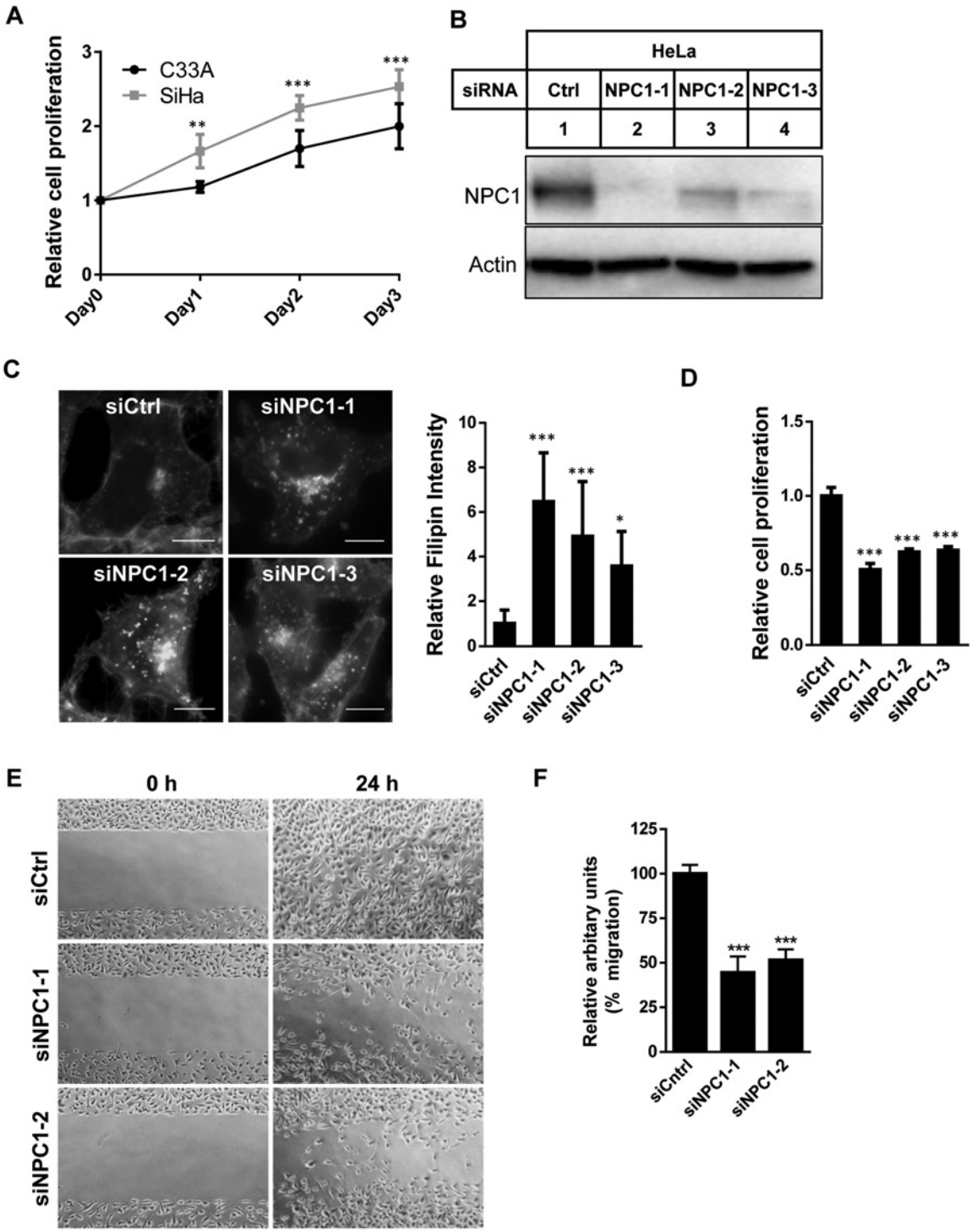

Figure 7 Depletion of NPC1 impairs the proliferation and migration of HeLa cells

(**A**) MTS colorimetric cell proliferation assay in C33A and SiHa cells grown for up to 3 days in 96-well plates. $^{**}P < 0.01$, $^{***}P < 0.001$, n=6. Results are representative of two independent experiments with similar results. (**B**) HeLa cells were treated with control siRNA or three different NPC1 siRNAs for 72 h and total cell lysates were analysed by immunoblotting to detect NPC1 and actin. (**C**) HeLa cells were treated with control siRNA or three different NPC1 siRNAs for 72 h, followed by processing for filipin staining for free cholesterol. Quantification of filipin intensity is shown in the right panel. (**D**) MTS colorimetric cell proliferation assay in control or NPC1 siRNA-treated HeLa cells as treated in (**A**) and (**B**). $^{***}P < 0.001$, n=12. Results are representative of three independent experiments with similar results. (**E** and **F**) HeLa cells were transfected with either control siRNA or two different NPC1 siRNAs for 24 h followed by a cell migration assay as described in the Experimental section. $^{***}P < 0.001$

growth observed in cancer [36] and importantly, both Akt signalling and NPC1 deficiency drives accumulation of cellular cholesterol [37,38]. In addition, NPC1 has been implicated in insulin signalling and insulin-induced Akt activation [39,40]. Compromised NPC1 levels or function was found to reduce insulin-stimulated Akt phosphorylation in adipocytes [39]. Consistent with this study, we found that NPC1 depletion impaired Akt activation induced by insulin in HepG2 cells (Supplementary Figure S5). Moreover, NPC1 down-regulation was reported to impair mTOR activation in endothelial cells [41]. We postulate that Akt/mTOR-mediated NPC1 degradation may provide a negative-feedback regulatory loop for the Akt pathway. Again, the key to this loop is cholesterol, which is essential for membrane expansion and the formation of signalling platforms in cholesterol-rich membrane domains [42]. With NPC1 being depleted, intracellular cholesterol trafficking is impaired and membrane cholesterol distribution is altered. This change in membrane cholesterol may interfere with growth factor-stimulated Akt/mTOR signalling [39,41]. In terms of cancer cell growth and survival, this negative-feedback regulatory loop may have important implications. We found that siRNA-mediated NPC1 depletion severely interfered with cell proliferation and migration in several cancer cell lines (Figure 7; Supplementary Figure S4). In cancer cells, the Akt pathway is usually activated for promoting cell growth and survival. However, when Akt is aberrantly activated, such as that in C33A cells and endometrial cancer cells, an adaptive mechanism may be developed to alleviate its effect. We propose that NPC1 down-regulation caused by Akt may be such a mechanism.

In summary, the findings of the present study uncover a role for the Akt/mTOR pathway in NPC1 degradation and a novel mechanism by which certain cancer cells accumulate high levels of cholesterol. Apart from being a master regulator of intracellular cholesterol transport, NPC1 has been implicated in many cellular and physiological processes, including atherosclerosis [43], insulin resistance [44–46], obesity [40,47] and virus infection [48–54]. Our results expand the roles of NPC1, linking this important cholesterol transport protein to optimal cancer cell proliferation and migration.

AUTHOR CONTRIBUTION

Ximing Du, Yuxi Zhang, and Hongyuan Yang conceived the project and designed the experiments. Ximing Du and Yuxi Zhang performed the main experiments and analyses. Sae Rom Jo mainly performed cell migration experiments. Xiaoyun Liu contributed to plasmid construction. Frances Byrne and Kyle Hoehn contributed to endometrial cancer cell experiments. Unpublished results, reagents, advice, design and supervision of experiments were provided by Yanfei Qi, Brenna Osborne, Greg Smith, Nigel Turner, and Andrew Brown. Manuscript was written by Ximing Du and Hongyuan Yang with input from Yuxi Zhang, Sae Rom Jo and Andrew Brown.

FUNDING

This work was supported by the National Health and Medical Research Council of Australia [grant number 1041301]. Hongyuan Yang is a Senior Research Fellow of the National Health and Medical Research Council (NHMRC) of Australia.

REFERENCES

1 Maceyka, M., Milstien, S. and Spiegel, S. (2013) The potential of histone deacetylase inhibitors in Niemann - Pick type C disease. FEBS J. **280**, 6367–6372 CrossRef PubMed
2 Patterson, M.C., Hendriksz, C.J., Walterfang, M., Sedel, F., Vanier, M.T., Wijburg, F. and Group, NP-C Guidelines Working Group. (2012) Recommendations for the diagnosis and management of Niemann-Pick disease type C: an update. Mol. Genet. Metab. **106**, 330–344 CrossRef PubMed
3 Carstea, E.D., Morris, J.A., Coleman, K.G., Loftus, S.K., Zhang, D., Cummings, C., Gu, J., Rosenfeld, M.A., Pavan, W.J., Krizman, D.B. et al. (1997) Niemann-Pick C1 disease gene: homology to mediators of cholesterol homeostasis. Science **277**, 228–231 CrossRef PubMed
4 Davies, J.P. and Ioannou, Y.A. (2000) Topological analysis of Niemann-Pick C1 protein reveals that the membrane orientation of the putative sterol-sensing domain is identical to those of 3-hydroxy-3-methylglutaryl-CoA reductase and sterol regulatory element binding protein cleavage-activating protein. J. Biol. Chem. **275**, 24367–24374 CrossRef PubMed
5 Scott, C., Higgins, M.E., Davies, J.P. and Ioannou, Y.A. (2004) Targeting of NPC1 to late endosomes involves multiple signals, including one residing within the putative sterol-sensing domain. J. Biol. Chem. **279**, 48214–48223 CrossRef PubMed
6 Liscum, L., Ruggiero, R.M. and Faust, J.R. (1989) The intracellular transport of low density lipoprotein-derived cholesterol is defective in Niemann-Pick type C fibroblasts. J. Cell Biol. **108**, 1625–1636 CrossRef PubMed
7 Vanier, M.T. (2010) Niemann-Pick disease type C. Orphanet J. Rare Dis. **5**, 16 CrossRef PubMed
8 Gelsthorpe, M.E., Baumann, N., Millard, E., Gale, S.E., Langmade, S.J., Schaffer, J.E. and Ory, D.S. (2008) Niemann-Pick type C1 I1061T mutant encodes a functional protein that is selected for endoplasmic reticulum-associated degradation due to protein misfolding. J. Biol. Chem. **283**, 8229–8236 CrossRef PubMed
9 Nakasone, N., Nakamura, Y.S., Higaki, K., Oumi, N., Ohno, K. and Ninomiya, H. (2014) Endoplasmic reticulum-associated degradation of Niemann-Pick C1: evidence for the role of heat shock proteins and identification of lysine residues that accept ubiquitin. J. Biol. Chem. **289**, 19714–19725 CrossRef PubMed
10 Sever, R. and Brugge, J.S. (2015) Signal transduction in cancer. Cold Spring Harb. Perspect. Med. **5**, a006098 CrossRef PubMed
11 Alessi, D.R., James, S.R., Downes, C.P., Holmes, A.B., Gaffney, P.R., Reese, C.B. and Cohen, P. (1997) Characterization of a 3-phosphoinositide-dependent protein kinase which phosphorylates and activates protein kinase Balpha. Curr. Biol. **7**, 261–269 CrossRef PubMed
12 Hresko, R.C. and Mueckler, M. (2005) mTOR.RICTOR is the Ser473 kinase for Akt/protein kinase B in 3T3-L1 adipocytes. J. Biol. Chem. **280**, 40406–40416 CrossRef PubMed
13 Sarbassov, D.D., Guertin, D.A., Ali, S.M. and Sabatini, D.M. (2005) Phosphorylation and regulation of Akt/PKB by the rictor-mTOR complex. Science **307**, 1098–1101 CrossRef PubMed
14 Manning, B.D. and Cantley, L.C. (2007) AKT/PKB signaling: navigating downstream. Cell **129**, 1261–1274 CrossRef PubMed
15 Krycer, J.R., Sharpe, L.J., Luu, W. and Brown, A.J. (2010) The Akt-SREBP nexus: cell signaling meets lipid metabolism. Trends Endocrinol. Metab. **21**, 268–276 CrossRef PubMed
16 Dimmeler, S., Fleming, I., Fisslthaler, B., Hermann, C., Busse, R. and Zeiher, A.M. (1999) Activation of nitric oxide synthase in endothelial cells by Akt-dependent phosphorylation. Nature **399**, 601–605 CrossRef PubMed
17 Ko, D.C., Gordon, M.D., Jin, J.Y. and Scott, M.P. (2001) Dynamic movements of organelles containing Niemann-Pick C1 protein: NPC1 involvement in late endocytic events. Mol. Biol. Cell **12**, 601–614 CrossRef PubMed
18 Du, X., Kumar, J., Ferguson, C., Schulz, T.A., Ong, Y.S., Hong, W., Prinz, W.A., Parton, R.G., Brown, A.J. and Yang, H. (2011) A role for oxysterol-binding protein-related protein 5 in endosomal cholesterol trafficking. J. Cell Biol. **192**, 121–135 CrossRef PubMed
19 Du, X., Kazim, A.S., Brown, A.J. and Yang, H. (2012) An essential role of Hrs/Vps27 in endosomal cholesterol trafficking. Cell Rep. **1**, 29–35 CrossRef PubMed
20 Rashmi, R., DeSelm, C., Helms, C., Bowcock, A., Rogers, B.E., Rader, J., Grigsby, P.W. and Schwarz, J.K. (2014) AKT inhibitors promote cell death in cervical cancer through disruption of mTOR signaling and glucose uptake. PLoS One **9**, e92948 CrossRef PubMed
21 Byrne, F.L., Poon, I.K., Modesitt, S.C., Tomsig, J.L., Chow, J.D., Healy, M.E., Baker, W.D., Atkins, K.A., Lancaster, J.M., Marchion, D.C. et al. (2014) Metabolic vulnerabilities in endometrial cancer. Cancer Res. **74**, 5832–5845 CrossRef PubMed
22 Liu, P., Begley, M., Michowski, W., Inuzuka, H., Ginzberg, M., Gao, D., Tsou, P., Gan, W., Papa, A., Kim, B.M. et al. (2014) Cell-cycle-regulated activation of Akt kinase by phosphorylation at its carboxyl terminus. Nature **508**, 541–545 CrossRef PubMed
23 Mairhofer, M., Steiner, M., Salzer, U. and Prohaska, R. (2009) Stomatin-like protein-1 interacts with stomatin and is targeted to late endosomes. J. Biol. Chem. **284**, 29218–29229 CrossRef PubMed
24 Takeuchi, K. and Reue, K. (2009) Biochemistry, physiology, and genetics of GPAT, AGPAT, and lipin enzymes in triglyceride synthesis. Am. J. Physiol. Endocrinol. Metab. **296**, E1195–E1209 CrossRef PubMed
25 Laplante, M. and Sabatini, D.M. (2012) mTOR signaling in growth control and disease. Cell **149**, 274–293 CrossRef PubMed
26 Hara, K., Maruki, Y., Long, X., Yoshino, K., Oshiro, N., Hidayat, S., Tokunaga, C., Avruch, J. and Yonezawa, K. (2002) Raptor, a binding partner of target of rapamycin (TOR), mediates TOR action. Cell **110**, 177–189 CrossRef PubMed

27 Sarbassov, D.D., Ali, S.M., Kim, D.H., Guertin, D.A., Latek, R.R., Erdjument-Bromage, H., Tempst, P. and Sabatini, D.M. (2004) Rictor, a novel binding partner of mTOR, defines a rapamycin-insensitive and raptor-independent pathway that regulates the cytoskeleton. Curr. Biol. **14**, 1296–1302 CrossRef PubMed

28 Sato, S., Ward, C.L., Krouse, M.E., Wine, J.J. and Kopito, R.R. (1996) Glycerol reverses the misfolding phenotype of the most common cystic fibrosis mutation. J. Biol. Chem. **271**, 635–638 CrossRef PubMed

29 Solomon, V.R. and Lee, H. (2009) Chloroquine and its analogs: a new promise of an old drug for effective and safe cancer therapies. Eur. J. Pharmacol. **625**, 220–233 CrossRef PubMed

30 Newton, A.C. and Trotman, L.C. (2014) Turning off AKT: PHLPP as a drug target. Annu. Rev. Pharmacol. Toxicol. **54**, 537–558 CrossRef PubMed

31 Dickey, C.A., Koren, J., Zhang, Y.J., Xu, Y.F., Jinwal, U.K., Birnbaum, M.J., Monks, B., Sun, M., Cheng, J.Q., Patterson, C. et al. (2008) Akt and CHIP coregulate tau degradation through coordinated interactions. Proc. Natl. Acad. Sci. U.S.A. **105**, 3622–3627 CrossRef PubMed

32 Brunet, A., Bonni, A., Zigmond, M.J., Lin, M.Z., Juo, P., Hu, L.S., Anderson, M.J., Arden, K.C., Blenis, J. and Greenberg, M.E. (1999) Akt promotes cell survival by phosphorylating and inhibiting a forkhead transcription factor. Cell **96**, 857–868 CrossRef PubMed

33 Manning, B.D., Tee, A.R., Logsdon, M.N., Blenis, J. and Cantley, L.C. (2002) Identification of the tuberous sclerosis complex-2 tumor suppressor gene product tuberin as a target of the phosphoinositide 3-kinase/akt pathway. Mol. Cell **10**, 151–162 CrossRef PubMed

34 Plas, D.R. and Thompson, C.B. (2003) Akt activation promotes degradation of tuberin and FOXO3a via the proteasome. J. Biol. Chem. **278**, 12361–12366 CrossRef PubMed

35 Kane, S., Sano, H., Liu, S.C., Asara, J.M., Lane, W.S., Garner, C.C. and Lienhard, G.E. (2002) A method to identify serine kinase substrates. Akt phosphorylates a novel adipocyte protein with a Rab GTPase-activating protein (GAP) domain. J. Biol. Chem. **277**, 22115–22118 CrossRef PubMed

36 Krycer, J.R. and Brown, A.J. (2013) Cholesterol accumulation in prostate cancer: a classic observation from a modern perspective. Biochim. Biophys. Acta **1835**, 219–229 PubMed

37 Du, X., Kristiana, I., Wong, J. and Brown, A.J. (2006) Involvement of Akt in ER-to-Golgi transport of SCAP/SREBP: a link between a key cell proliferative pathway and membrane synthesis. Mol. Biol. Cell **17**, 2735–2745 CrossRef PubMed

38 Kristiana, I., Yang, H. and Brown, A.J. (2008) Different kinetics of cholesterol delivery to components of the cholesterol homeostatic machinery: implications for cholesterol trafficking to the endoplasmic reticulum. Biochim. Biophys. Acta **1781**, 724–730 CrossRef PubMed

39 Fletcher, R., Gribben, C., Ma, X., Burchfield, J.G., Thomas, K.C., Krycer, J.R., James, D.E. and Fazakerley, D.J. (2014) The role of the Niemann-Pick disease, type c1 protein in adipocyte insulin action. PLoS One **9**, e95598 CrossRef PubMed

40 Jelinek, D., Millward, V., Birdi, A., Trouard, T.P., Heidenreich, R.A. and Garver, W.S. (2011) Npc1 haploinsufficiency promotes weight gain and metabolic features associated with insulin resistance. Hum. Mol. Genet. **20**, 312–321 CrossRef PubMed

41 Xu, J., Dang, Y., Ren, Y.R. and Liu, J.O. (2010) Cholesterol trafficking is required for mTOR activation in endothelial cells. Proc. Natl. Acad. Sci. U.S.A. **107**, 4764–4769 CrossRef PubMed

42 Sheng, R., Chen, Y., Yung Gee, H., Stec, E., Melowic, H.R., Blatner, N.R., Tun, M.P., Kim, Y., Kallberg, M., Fujiwara, T.K. et al. (2012) Cholesterol modulates cell signaling and protein networking by specifically interacting with PDZ domain-containing scaffold proteins. Nat. Commun. **3**, 1249 CrossRef PubMed

43 Zhang, J.R., Coleman, T., Langmade, S.J., Scherrer, D.E., Lane, L., Lanier, M.H., Feng, C., Sands, M.S., Schaffer, J.E., Semenkovich, C.F. and Ory, D.S. (2008) Niemann-Pick C1 protects against atherosclerosis in mice via regulation of macrophage intracellular cholesterol trafficking. J. Clin. Invest. **118**, 2281–2290 PubMed

44 Nomura, M., Ishii, H., Kawakami, A. and Yoshida, M. (2009) Inhibition of hepatic Niemann-Pick C1-like 1 improves hepatic insulin resistance. Am. J. Physiol. Endocrinol. Metab. **297**, E1030–E1038 CrossRef PubMed

45 Ong, Q.R., Lim, M.L., Chua, C.C., Cheung, N.S. and Wong, B.S. (2012) Impaired insulin signaling in an animal model of Niemann-Pick type C disease. Biochem. Biophys. Res. Commun. **424**, 482–487 CrossRef PubMed

46 Vainio, S., Bykov, I., Hermansson, M., Jokitalo, E., Somerharju, P. and Ikonen, E. (2005) Defective insulin receptor activation and altered lipid rafts in Niemann-Pick type C disease hepatocytes. Biochem. J. **391**, 465–472 CrossRef PubMed

47 Borbon, I., Campbell, E., Ke, W. and Erickson, R.P. (2012) The role of decreased levels of Niemann-Pick C1 intracellular cholesterol transport on obesity is reversed in the C57BL/6J, metabolic syndrome mouse strain: a metabolic or an inflammatory effect? J. Appl. Genet. **53**, 323–330 CrossRef PubMed

48 Jupatanakul, N., Sim, S. and Dimopoulos, G. (2014) *Aedes aegypti* ML and Niemann-Pick type C family members are agonists of dengue virus infection. Dev. Comp. Immunol. **43**, 1–9 CrossRef PubMed

49 Sainz, Jr, B., Barretto, N., Martin, D.N., Hiraga, N., Imamura, M., Hussain, S., Marsh, K.A., Yu, X., Chayama, K., Alrefai, W.A. and Uprichard, S.L. (2012) Identification of the Niemann-Pick C1-like 1 cholesterol absorption receptor as a new hepatitis C virus entry factor. Nat. Med. **18**, 281–285 CrossRef PubMed

50 Tang, Y., Leao, I.C., Coleman, E.M., Broughton, R.S. and Hildreth, J.E. (2009) Deficiency of niemann-pick type C-1 protein impairs release of human immunodeficiency virus type 1 and results in Gag accumulation in late endosomal/lysosomal compartments. J. Virol. **83**, 7982–7995 CrossRef PubMed

51 Carette, J.E., Raaben, M., Wong, A.C., Herbert, A.S., Obernosterer, G., Mulherkar, N., Kuehne, A.I., Kranzusch, P.J., Griffin, A.M., Ruthel, G. et al. (2011) Ebola virus entry requires the cholesterol transporter Niemann-Pick C1. Nature **477**, 340–343 CrossRef PubMed

52 Cote, M., Misasi, J., Ren, T., Bruchez, A., Lee, K., Filone, C.M., Hensley, L., Li, Q., Ory, D., Chandran, K. and Cunningham, J. (2011) Small molecule inhibitors reveal Niemann-Pick C1 is essential for Ebola virus infection. Nature **477**, 344–348 CrossRef PubMed

53 Lee, K., Ren, T., Cote, M., Gholamreza, B., Misasi, J., Bruchez, A. and Cunningham, J. (2013) Inhibition of Ebola virus infection: identification of Niemann-Pick C1 as the target by optimization of a chemical probe. ACS Med. Chem. Lett. **4**, 239–243 CrossRef PubMed

54 Shoemaker, C.J., Schornberg, K.L., Delos, S.E., Scully, C., Pajouhesh, H., Olinger, G.G., Johansen, L.M. and White, J.M. (2013) Multiple cationic amphiphiles induce a Niemann-Pick C phenotype and inhibit Ebola virus entry and infection. PLoS One **8**, e56265 CrossRef PubMed

Received 26 May 2015/12 August 2015; accepted 17 August 2015
Accepted Manuscript online 17 August 2015, doi:10.1042/BJ20150602